Journal of Sound and Vibration (1999) **228**(5), 1103–1124
Article No. jsvi.1999.2476, available online at http://www.idealibrary.com on IDEAL®

NON-LINEAR DYNAMICS AND STABILITY OF CIRCULAR CYLINDRICAL SHELLS CONTAINING FLOWING FLUID, PART II: LARGE-AMPLITUDE VIBRATIONS WITHOUT FLOW

M. AMABILI

Dipartimento di Ingegneria Industriale, Università di Parma, Viale delle Scienze, Parma, I-43100 Italy

F. PELLICANO

Dipartimento di Scienze dell'Ingegneria, Università di Modena e Reggio Emilia, Via Campi 213b, Modena, I-41100 Italy

AND

M. P. PAÏDOUSSIS

Department of Mechanical Engineering, McGill University, 817 Sherbrooke Street W., Montréal, Québec H3A 2K6, Canada

(*Received* 24 *February* 1999, *and in final form* 21 *June* 1999)

The non-linear response of empty and fluid-filled circular cylindrical shells to harmonic excitations is investigated. Both modal and point excitations have been considered. The model is suitable to study simply supported shells with and without axial constraints. Donnell's non-linear shallow-shell theory is used. The boundary conditions on radial displacement and the continuity of circumferential displacement are exactly satisfied. The radial deflection of the shell is expanded by using a basis of seven linear modes. The effect of internal quiescent, incompressible and inviscid fluid is investigated. The equations of motion, obtained in Part I of this study, are studied by using a code based on the collocation method. The validation of the present model is obtained by comparison with other authoritative results. The effect of the number of axisymmetric modes used in the expansion on the response of the shell is investigated, clarifying questions open for a long time. The results show the occurrence of travelling wave response in the proximity of the resonance frequency, the fundamental role of the first and third axisymmetric modes in the expansion of the radial deflection with one longitudinal half-wave, and limit cycle responses. Modes with two longitudinal half-waves are also investigated.

1. INTRODUCTION

The large-amplitude vibrations of circular cylindrical shells have interested many researchers in the last 40 years, as a consequence of the wide applications of these elements in engineering. Even though the study of this problem has a long tradition, several questions still await for complete clarification. In the past, some discussions between leading authors have been published in the *Journal of Sound and Vibration*; others have recently been published in the *Journal of Fluids and Structures* [1–3], testifying that the topic still presents open questions.

A full literature review of work on the non-linear dynamics of shells *in vacuo* and filled with or surrounded by quiescent fluid is given by Amabili *et al.* [4] and will not be repeated here. However, it is necessary to refer to some fundamental and some recent contributions. Briefly, it is possible to attribute to Evensen [5] and Dowell and Ventres [6] the original idea of mode expansions of the flexural displacement involving the linear mode considered, the companion mode and an axisymmetric term; their intuition was supported by a few available experimental results. The studies of Ginsberg [7] and Chen and Babcock [8] constitute fundamental contributions to the study of the influence of the companion mode on the non-linear forced response of circular cylindrical shells. Ginsberg [7] employed an expansion involving ideally all the linear modes plus an axial displacement to satisfy the non-linear boundary conditions. He found that the fundamental terms in the expansion of the radial displacement are: the excited mode, the companion mode, all the axisymmetric modes with an odd number of axial half-waves, plus the modes with a circumferential wavenumber twice those being excited. Chen and Babcock [8] used a sophisticated mode expansion, including boundary layer terms, in order to satisfy the non-linear boundary conditions. Ganapathi and Varadan [9] studied the free response by using the finite-element method. Gonçalves and Batista [10] and Amabili *et al.* [4] studied the response of fluid-filled shells. In particular, Gonçalves and Batista [10] neglected the companion mode participation, the importance of which in the non-linear response was investigated by Amabili *et al.* [4].

Available studies show that a linear modal base is the simplest choice to discretize the system. In particular, in order to reduce the number of degrees of freedom (d.o.f.), it is important to use only the most significant modes. Most of the studies consider, in addition to the regular or "driven" asymmetric mode under consideration and the corresponding companion mode, also some axisymmetric modes. In fact, it has clearly been established that, for non-linear shell vibrations, the deformation of the shell involves a significant axisymmetric contraction of the circumference. It has never been clarified how many axisymmetric terms are necessary to obtain a good accuracy in the model. It is now believed [1, 2] that their number is important in predicting the kind of softening behaviour that has been observed in the experiments.

This is the second in a series of papers in which the non-linear dynamics of shells is reconsidered. The raison d'être of this new series of studies is that the problem is reanalyzed (i) using a fuller and more appropriate modal basis and (ii) fully satisfying continuity of circumferential displacement. The work presented in reference [4] represents a seminal contribution in this direction, more fully exploited in this current series of papers. A fuller discussion of the rationale for these studies may be found in reference [2].

The non-linear forced vibrations of a simply supported, circular cylindrical shell filled with an incompressible and inviscid, quiescent and dense fluid are investigated. The equations of motion obtained in Part I of the present study [11] are used. They have been obtained by using Donnell's non-linear shallow-shell theory. The boundary conditions on radial displacement and the continuity of circumferential displacement are exactly satisfied, while axial constraints are satisfied on the average. Both modal excitations and point excitations are considered.

The radial displacement of the shell is expanded by using a basis of seven linear modes; in particular, three axisymmetric modes with an odd number of axial half-waves are employed. The equations of motion obtained by Amabili *et al.* [11] are suitable for the study of modes of up to two axial half-waves.

The equations of motion are studied by using a code based on the collocation method. Numerical results are obtained for forced vibrations of empty and water-filled shells. In particular, results obtained with a different number of axisymmetric modes (with an odd number of axial half-waves) in the expansion of the radial displacement are compared, in order to clarify definitively this effect on the accuracy of the model. It is found that the resonant frequency is a function of the amplitude of vibration, generally displaying a softening behaviour, when two or more axisymmetric modes (with an odd number of axial half-waves) are employed.

2. EXTERNAL HARMONIC EXCITATION

In Part I of the present study [11], an external modal excitation f of unspecified physical origin was assumed, as follows:

$$f = f_n \cos(n\theta) \sin(\pi x/L) \cos(\omega t), \tag{1}$$

where n is the number of circumferential waves, L the shell length, ω the radian frequency of the excitation, x the axial co-ordinate, θ the angular co-ordinate, and t the time. Although this was part of the formulation, in the numerical calculations $f_n = 0$ was always used, where f_n is the excitation amplitude, since Part I was concerned with the stability of free motions of the shell subjected to internal flow. The Galerkin projection of the modal excitation f on the weighting functions z_s, $s = 1, \ldots, 7$, gives [11]

$$\langle f, z_s \rangle = \begin{cases} \dfrac{\pi L}{2} f_{1,n} \cos(\omega t) & \text{for } s = 1, \\ 0 & \text{for } s \neq 1. \end{cases} \tag{2}$$

Therefore, the modal excitation gives a non-zero contribution only to the driven mode. This kind of excitation is quite unrealistic. Practically, one has to deal with one or more forces applied to the system. More realistic is the case of a harmonic point excitation, modelling for instance the excitation by an electrodynamical exciter (shaker); this could be suitable for comparison with experimental results. The point excitation can be described by the following expression:

$$f = \tilde{f} \delta(\theta - \tilde{\theta}) \delta(x - \tilde{x}) \cos(\omega t), \tag{3}$$

where δ is the Dirac delta function, $\tilde{f}$ the excitation amplitude, $\tilde{\theta}$ and $\tilde{x}$ the angular and axial position of the point of application of the force, respectively; here, the point excitation is located at $\tilde{\theta} = 0$, $\tilde{x} = L/2$. The Galerkin projection of the point excitation f on the weighting functions z_s, $s = 1, \ldots, 7$, gives

$$\langle f, z_s \rangle = \begin{cases} \tilde{f}\cos(\omega t) & \text{for } s = 1, 5, 6, 7, \\ 0 & \text{for } s = 2, 3, 4. \end{cases} \tag{4}$$

Setting $\tilde{f} = f_{1,n}\pi L/2$, the only difference between equation (2) and equation (4) is that the point excitation directly drives also the axisymmetric modes.

3. SHELLS VIBRATING *IN VACUO*: RESULTS AND DISCUSSION

All the numerical results have been obtained by using the software *AUTO* [12] for bifurcation and continuation of ordinary differential equations, based on a collocation method. The periodical results obtained are reported, showing the maximum or minimum amplitude of the generalized co-ordinates in the period. The generalized co-ordinates are related to the basis of linear modes used in the expansion of the radial displacement w as follows [11]: $A_{1,n}(t)$, first longitudinal driven mode; $B_{1,n}(t)$, first longitudinal companion mode; $A_{2,n}(t)$, second longitudinal driven mode; $B_{2,n}(t)$, second longitudinal companion mode; $A_{1,0}(t)$, first axisymmetric mode; $A_{3,0}(t)$, third axisymmetric mode; $A_{5,0}(t)$, fifth axisymmetric mode. The oscillation amplitude of these variables is normalized by the shell thickness h for easy interpretation of the results.

The case analyzed here was studied by Chen and Babcock [8] and it relates to a circular cylindrical shell in vacuum, simply supported at the ends (with zero axial force N_x), and having the following dimensions and properties: $L = 0{\cdot}2$ m, $R = 0{\cdot}1$ m, $h = 0{\cdot}247 \times 10^{-3}$ m, $E = 71{\cdot}02 \times 10^9$ Pa, $\rho = 2796$ kg/m^3 and $\nu = 0{\cdot}31$; the mode investigated is $n = 6$ and $m = 1$ and 2 (where m is the number of longitudinal half-waves). Chen and Babcock [8] studied only the case with $m = 1$. It is interesting to note that, for symmetry reasons, the second longitudinal mode is not coupled to the first one. Therefore, the model developed in Part I of the present study [11] can be reduced to one of five d.o.f. by imposing $A_{2,n}(t) = B_{2,n}(t) = 0$ for $m = 1$ and $A_{1,n}(t) = B_{1,n}(t) = 0$ for $m = 2$.

The response-frequency relationship (computed by using the 5 d.o.f. model) of the driven mode without companion mode participation ($B_{1,n}(t) = 0$) for $m = 1$, is shown in Figure 1; the present results (continuous line) are compared with those analytically obtained by Chen and Babcock [8] (dashed lines) and Amabili *et al.* [4] (chain-dotted line) for an amplitude of the external modal excitation of $f_{1,n} = 0{\cdot}0012 h^2 \rho \omega_{1,n}^2$ and a damping ratio $2\zeta_{1,n} = 0{\cdot}001$ (with $\zeta_{1,0} = \zeta_{1,n}\omega_{1,0}/\omega_{1,n}$ and $\zeta_{3,0} = \zeta_{1,n}\ \omega_{3,0}/\omega_{1,n}$); the linear radian frequencies are $\omega_{1,n} = 2\pi \times 564{\cdot}2$, $\omega_{1,0} = 2\pi \times 8021$, $\omega_{3,0} = 2\pi \times 8023$ and $\omega_{5,0} = 2\pi \times 8030$ rad/s. The backbone curves (pertaining to undamped free vibrations) are also shown in this figure. Figure 1 shows reasonably good agreement between the present results and those obtained theoretically by Chen and Babcock [8] and Amabili *et al.* [4]. The same case was also studied by Ganapathi and Varadan [9], only for free vibrations; they

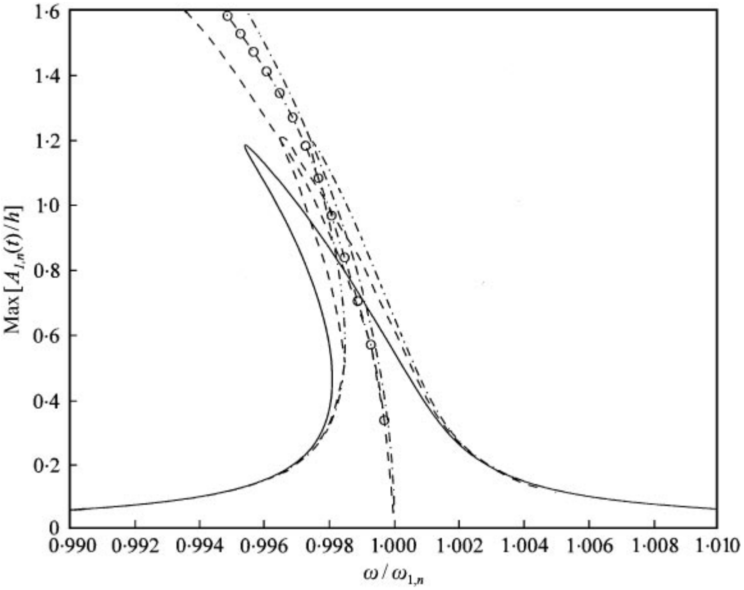

Figure 1. Frequency-response curves and backbone curves for the driven mode without companion mode participation, $m = 1$: ——, present results; ·–·–·, Amabili *et al.* [4]; – – –, Chen and Babcock [8]; –○– the backbone curve of Ganapathi and Varadan [9].

obtained a backbone curve, also shown in Figure 1, in reasonably good agreement with the present results. The non-linearity is of the softening type in Figure 1.

Particularly interesting is the comparison between the present result, obtained with a 5 d.o.f. model, and the curve of Amabili *et al.* [4], obtained with a 3 d.o.f model (in this case a kinematic constraint between the first two axisymmetric modes considered was used to reduce the d.o.f. to 3). The present model gives more strongly softening results than that presented by Amabili *et al.* [4], as a consequence of the removal of this artificial constraint and the introduction of a fifth axisymmetric mode.

3.1. COMPARISON OF DIFFERENT MODELS

A question that is still open is the effect of the number of axisymmetric modes that needs to be retained in the expansion of the flexural displacement on the non-linear response of closed, circular shells. Generally, hardening-type results were found in calculations in which only the first axisymmetric mode was retained, e.g., by Atluri [13], who followed the model of Dowell and Ventres [6]. Varadan *et al.* [14] showed that retaining only the first axisymmetric mode gives hardening-type results, whereas the mode expansion of Evensen [5] gives softening-type results for the same case. In particular, the axisymmetric term used by Evensen [5] is not a true axisymmetric mode, but it is obtained by satisfying exactly the continuity of the circumferential displacement; however, it does not satisfy the moment-free boundary condition at the shell edges. Amabili *et al.* [4] obtained

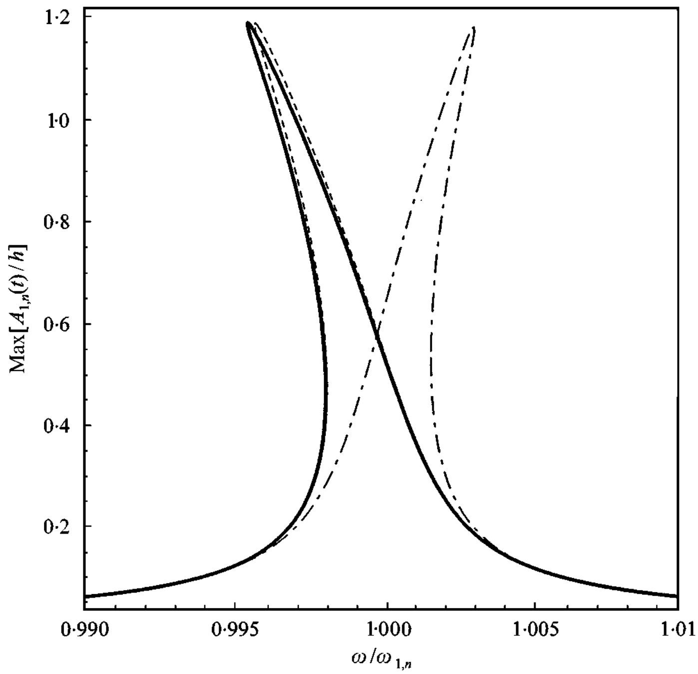

Figure 2. Frequency-response curves for the driven mode without companion mode participation, $m = 1$: ——, model with 3 axisymmetric modes; – – –, model 2 axisymmetric modes; · –· – ·, model with 1 axisymmetric mode.

results in good agreement with other authoritative published results by using an expansion involving the first and third axisymmetric modes joined by an artificial kinematic constraint to reduce the number of d.o.f. to 3. They also introduced an improved homogeneous solution *vis-à-vis* those used in the past, e.g., in references [6, 13]. It is therefore of considerable interest to understand the reason for obtaining such different results with a one-axisymmetric-mode expansion [13], on the one hand, and those of Evensen [5] and Amabili *et al.* [4], on the other.

In order to explain the effect of axisymmetric modes on the response of the shell, Figure 2 shows the frequency-response relationship of the driven mode without companion mode participation, computed with three axisymmetric modes (continuous line), two axisymmetric modes (dashed line) and with only the first axisymmetric mode (chain-dotted line). It is very interesting to observe that the models with 2 and 3 axisymmetric modes give results very close to each other, whereas the model with only the first axisymmetric mode gives a completely different result, showing the opposite trend of non-linearity. It should be noted that the amplitude of the first axisymmetric mode is the same in the three models. This result effectively explains the reason for the hardening-type results obtained by Atluri [13] and Varadan *et al.* [14] with the model initially proposed by Dowell and Ventres [6]: not only the first but also the third axisymmetric mode is evidently fundamental for the adequate description of the non-linear response of closed, circular shells. Further discussion is deferred to sections 3.2 and 3.3, where the equations of motion and the response of all generalized co-ordinates are discussed.

As a consequence of the closeness of the responses computed with 2 and 3 axisymmetric modes, it is reasonably believed that a further increase of the number of axisymmetric modes (i.e., d.o.f.s.) to the present model does not give a significant change to the response of this system.

3.2. ACCURACY OF DIFFERENT MODELS FROM CONSIDERATION ON THE EQUATIONS OF MOTION

The equations of motion have been obtained in Part I of this study [11]. It is useful to rewrite these here in non-dimensional form, by introducing the following parameters:

$$\begin{gathered}\tau = \omega_{1,n}t, \qquad \tilde{A}_{1,n}(\tau) = A_{1,n}(\tau)/h, \qquad \tilde{B}_{1,n}(\tau) = B_{1,n}(\tau)/h,\\ \tilde{A}_{1,0}(\tau) = A_{1,0}(\tau)/h, \qquad \tilde{A}_{3,0}(\tau) = A_{3,0}(\tau)/h, \quad \tilde{A}_{5,0}(\tau) = A_{5,0}(\tau)/h.\end{gathered} \tag{5}$$

The case of $m = 1$ is now being studied so that it is possible to set $A_{2,n}(t) = B_{2,n}(t) = 0$. In particular, equations (46a, e–g) of Part I [11], related to the driven and axisymmetric modes, can be transformed as follows:

$$\begin{aligned}&\ddot{\tilde{A}}_{1,n}(\tau) + 2\zeta_{1,n}\dot{\tilde{A}}_{1,n}(\tau) + \tilde{A}_{1,n}(\tau) + \tilde{h}_1\tilde{A}^3_{1,n}(\tau) + \tilde{h}_1\tilde{A}_{1,n}(\tau)\tilde{B}^2_{1,n}(\tau)\\ &\quad + \tilde{h}_5\tilde{A}_{1,n}(\tau)\tilde{A}_{1,0}(\tau) + \tilde{h}_6\tilde{A}_{1,n}(\tau)\tilde{A}_{3,0}(\tau) + \tilde{h}_7\tilde{A}_{1,n}(\tau)\tilde{A}_{5,0}(\tau) + \tilde{h}_8\tilde{A}_{1,n}(\tau)\tilde{A}^2_{1,0}(\tau)\\ &\quad + \tilde{h}_9\tilde{A}_{1,n}(\tau)\tilde{A}^2_{3,0}(\tau) + \tilde{h}_{10}\tilde{A}_{1,n}(\tau)\tilde{A}^2_{5,0}(\tau) + \tilde{h}_{11}\tilde{A}_{1,n}(\tau)\tilde{A}_{1,0}(\tau)\tilde{A}_{3,0}(\tau)\\ &\quad + \tilde{h}_{12}\tilde{A}_{1,n}(\tau)\tilde{A}_{3,0}(\tau)\tilde{A}_{5,0}(\tau) = [f_{1,n}/(h^2\rho\omega^2_{1,n})]\cos(\omega\tau/\omega_{1,n}),\end{aligned} \tag{6}$$

$$\begin{aligned}&\ddot{\tilde{A}}_{1,0}(\tau) + 2\zeta_{1,0}\omega_{1,0}\dot{\tilde{A}}_{1,0}(\tau) + (\omega_{1,0}/\omega_{1,n})^2\tilde{A}_{1,0}(\tau) + \tilde{l}_1\tilde{A}_{1,0}(\tau)\tilde{A}^2_{1,n}(\tau)\\ &\quad + \tilde{l}_1\tilde{A}_{1,0}(\tau)\tilde{B}^2_{1,n}(\tau) + \tilde{l}_3\tilde{A}^2_{1,n}(\tau) + \tilde{l}_3\tilde{B}^2_{1,n}(\tau) + \tilde{l}_5\tilde{A}_{3,0}(\tau)\tilde{A}^2_{1,n}(\tau)\\ &\quad + \tilde{l}_5\tilde{A}_{3,0}(\tau)\tilde{B}^2_{1,n}(\tau) = 0,\end{aligned} \tag{7}$$

$$\begin{aligned}&\ddot{\tilde{A}}_{3,0}(\tau) + 2\zeta_{3,0}\omega_{3,0}\dot{\tilde{A}}_{3,0}(\tau) + (\omega_{3,0}/\omega_{1,n})^2\tilde{A}_{3,0}(\tau) + \tilde{n}_1\tilde{A}_{3,0}(\tau)\tilde{A}^2_{1,n}(\tau)\\ &\quad + \tilde{n}_1\tilde{A}_{3,0}(\tau)\tilde{B}^2_{1,n}(\tau) + \tilde{n}_3\tilde{A}^2_{1,n}(\tau) + \tilde{n}_3\tilde{B}^2_{1,n}(\tau) + \tilde{n}_5\tilde{A}_{1,0}(\tau)\tilde{A}^2_{1,n}(\tau)\\ &\quad + \tilde{n}_5\tilde{A}_{1,0}(\tau)\tilde{B}^2_{1,n}(\tau) + \tilde{n}_7\tilde{A}_{5,0}(\tau)\tilde{A}^2_{1,n}(\tau) + \tilde{n}_7\tilde{A}_{5,0}(\tau)\tilde{B}^2_{1,n}(\tau) = 0,\end{aligned} \tag{8}$$

$$\begin{aligned}&\ddot{\tilde{A}}_{5,0}(\tau) + 2\zeta_{5,0}\omega_{5,0}\dot{\tilde{A}}_{5,0}(\tau) + (\omega_{5,0}/\omega_{1,n})^2\tilde{A}_{5,0}(\tau) + \tilde{p}_1\tilde{A}_{5,0}(\tau)\tilde{A}^2_{1,n}(\tau)\\ &\quad + \tilde{p}_1\tilde{A}_{5,0}(\tau)\tilde{B}^2_{1,n}(\tau) + \tilde{p}_3\tilde{A}^2_{1,n}(\tau) + \tilde{p}_3\tilde{B}^2_{1,n}(\tau) + \tilde{p}_6\tilde{A}_{3,0}(\tau)\tilde{A}^2_{1,n}(\tau)\\ &\quad + \tilde{p}_6\tilde{A}_{3,0}(\tau)\tilde{B}^2_{1,n}(\tau) = 0,\end{aligned} \tag{9}$$

where $\tilde{h}_i$ for $i = 1, \ldots, 12$, $\tilde{l}_i$ for $i = 1, \ldots, 5$, $\tilde{n}_i$ for $i = 1, \ldots, 7$, and $\tilde{p}_i$ for $i = 1, \ldots, 6$, are appropriate coefficients. It is very interesting to note that the quadratic terms in equation (6) involve products of $\tilde{A}_{1,n}(\tau)$ only, multiplied by the generalized co-ordinates associated with axisymmetric modes. These terms are essential for determining the trend of non-linearity in the frequency-response relationship.

In order to understand fully the numerical results presented in Figure 2 and the role of axisymmetric terms in the characterization of the type of non-linearity in the

7 d.o.f. model, the equations of motion (6–9) are studied analytically by means of a perturbation procedure described in detail in reference [4] for a simpler model. For the sake of brevity, the analytical developments are skipped and only the analytical expression of the non-linear, non-dimensional free oscillation frequency, for single-mode response, is given here:

$$\hat{\omega}_1 = \omega_1 + \beta a_1^2 + O(a_1^3), \tag{10}$$

where $\omega_1 = \omega_{1,n}/\omega_{1,n} = 1$, $a_1 = |A_{1,n}|/(2h)$ and

$$\beta = \frac{1}{4\omega_1}\left(6\tilde{h}_1 + \frac{2\tilde{h}_5\tilde{l}_3(8\omega_1^2 - 3\omega_5^2)}{-4\omega_1^2\omega_5^2 + \omega_5^4} - \frac{4\tilde{h}_6\tilde{n}_3}{\omega_6^2} + \frac{2\tilde{h}_6\tilde{n}_3}{4\omega_1^2 - \omega_6^2} - \frac{4\tilde{h}_7\tilde{p}_3}{\omega_7^2}\frac{2\tilde{h}_7\tilde{p}_3}{4\omega_1^2 - \omega_7^2}\right). \tag{11}$$

For the case under study, the coefficients used in equations (6–9) are

$$\tilde{h}_1 = 0{\cdot}300378, \quad \tilde{h}_5 = -15{\cdot}3696, \quad \tilde{h}_6 = 3{\cdot}4456, \quad \tilde{h}_7 = 0{\cdot}692128,$$

$$\tilde{l}_3 = -3{\cdot}84706, \quad \tilde{n}_3 = 0{\cdot}8196, \quad \tilde{p}_3 = 0{\cdot}131, \quad \omega_5 = \omega_{1,0}/\omega_{1,n} = 14{\cdot}22,$$

$$\omega_6 = \omega_{3,0}/\omega_{1,n} = 14{\cdot}22, \quad \omega_7 = \omega_{5,0}/\omega_{1,n} = 14{\cdot}23.$$

The sign of the coefficient β given in equation (10) characterizes the type of non-linearity: minus for softening, and plus for hardening non-linearity; the absolute value quantifies the effectiveness of the non-linearity itself. Equations (10) and (11) can also be used in approaching the problem with fewer d.o.f.s. In particular, reduced models are obtained by eliminating axisymmetric terms in the equations of motion and by assuming some coefficients to be equal to zero in equation (11). In Table 1, values of the coefficient β are evaluated for four different models: (i) no axisymmetric terms ($n = 0$) are involved in the expansion, i.e., $\tilde{h}_5$, $\tilde{h}_6, \tilde{h}_7, \tilde{l}_3, \tilde{n}_3, \tilde{p}_3$ are assumed to be equal to zero; (ii) only the first axisymmetric mode ($n = 0$, $m = 1$) is considered, i.e., $\tilde{h}_6, \tilde{h}_7, \tilde{n}_3, \tilde{p}_3$ are assumed to be equal to zero; (iii) only the first and the third ($n = 0$, $m = 3$) axisymmetric modes are considered, i.e., $\tilde{h}_7, \tilde{p}_3$ are assumed to be equal to zero; (iv) all the modes are retained, i.e., all the seven (actually five for driven mode with $m = 1$, as previously discussed) d.o.f.s. are used. The results in Table 1 suggest that the axisymmetric terms ($n = 0$) give a softening contribution which counters the hardening contribution of asymmetric terms ($n > 0$). The contribution of the first axisymmetric term is not sufficient to balance the hardening effect of asymmetric terms, and the third axisymmetric term is needed to calculate the correct trend of

TABLE 1

Values of coefficient β, giving the trend of non-linearity, for four different models. Model 1: *no axisymmetric modes*; *model* 2: *first axisymmetric mode only*; *model* 3: *first and third axisymmetric modes*; *model* 4: *first, third and fifth axisymmetric modes*

Model 1	Model 2	Model 3	Model 4
0·45	0·00883	– 0·01226	– 0·01294

non-linearity. The fifth axisymmetric term seems to give a very small contribution, showing that the convergence of the transverse displacement expansion is almost reached when retaining two axisymmetric terms. Note that the foregoing comments apply to single-mode response without excitation of other asymmetric modes or presence of internal resonances.

3.3. RESULTS FROM THE COMPLETE MODEL

Figures 3 and 4 show the frequency-response relationship when all the five d.o.f.s are active and indicate the stability of the solution for $m = 1$; both the maximum, Figure 3, and minimum, Figure 4, amplitude of each generalized co-ordinate during the oscillation period are shown. The oscillations of some variables often have a mean value different from zero.

It is interesting to observe in Figures 3(a) and 4(a) that, as a consequence of the appearance of the companion mode ($B_{1,n}(t) \neq 0$), only a small part of the solution is stable near the resonant part (peak) of the response of the driven mode. The rest of the stable response curve has an amplitude much smaller than that predicted without the participation of companion mode. The amplitude of the companion mode is shown in Figures 3(b) and 4(b) and has almost the same magnitude as the stable response of the driven mode, excluding the small stable portion near the tip of the curve in Figures 3(a) and 4(a). Figures 3(c–e) and 4(c–e) are of interest because they show the behaviour of the axisymmetric modes, the effect of which on shell response has been investigated in section 3.1. It is observed that Figures 3(d, e) and 4(d, e) are qualitatively similar, while Figures 3(c) and 4(c) have opposite signs. This is a reason for the necessity of including both the first and third axisymmetric modes in the expansion of the flexural displacement, as previously discussed. It is also interesting to note that the axisymmetric modes oscillate with a mean value significantly different from zero; this mean value has an opposite sign for the first and the other axisymmetric modes.

The difference between a modal excitation and a point excitation has been found to be negligible for the case under investigation; the frequency-response relationship obtained with point excitation is almost coincident with the one given in Figures 3 and 4. This result can easily be justified by observing that the linear frequencies of the axisymmetric modes are in this case very far from the linear frequency of the driven mode. Therefore, the response of axisymmetric modes under direct excitation at a frequency very far from their resonance is negligible.

The frequency-response relationship for the case $m = 2$ is shown in Figure 5. It is noted that results for the non-linear shell response in modes with $m > 1$ are very rare in the literature and their accuracy is uncertain. Comparison of Figures 3 and 5 shows that the response for $m = 2$ displays a slightly increased softening non-linearity with respect to $m = 1$. Moreover, Figures 5(c) and (d) are similar to Figure 3(c); Figure 5(e) is similar to Figures 3(d) and (e). Therefore, the transition from one type of response to the other is deferred to the successive odd axisymmetric mode in the case of $m = 2$. This result indicates that, for modes with two longitudinal half-waves ($m = 2$), the fifth axisymmetric mode is fundamental for predicting the

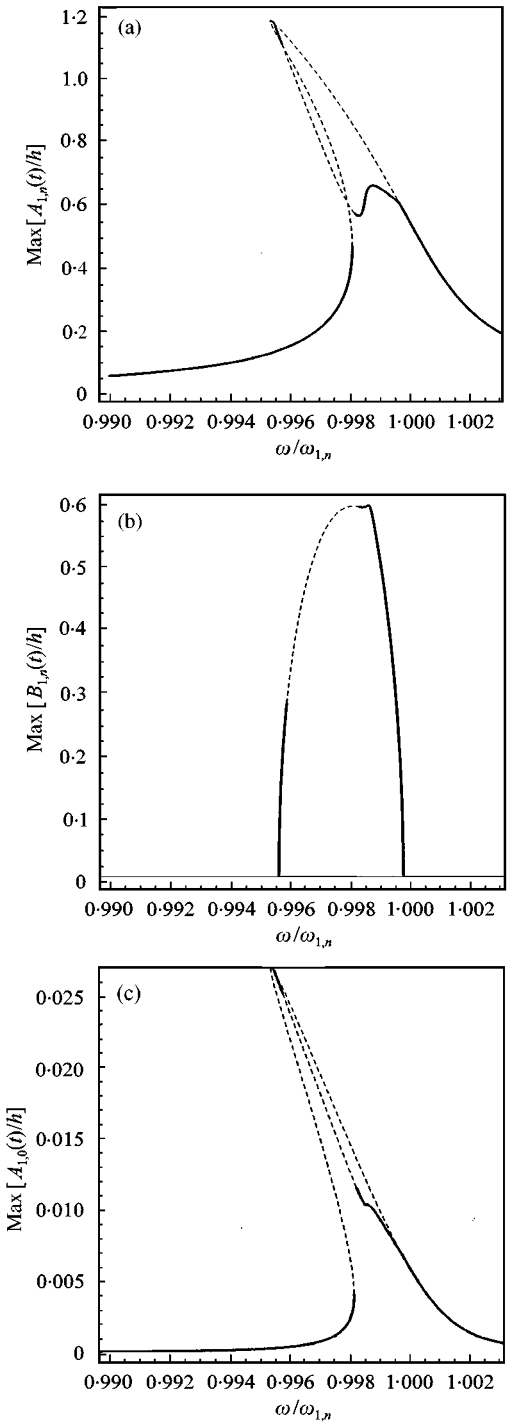

Figure 3. Frequency-response curve with companion mode participation, $m = 1$. (a) Maximum of $A_{1,n}(t)/h$; (b) maximum of $B_{1,n}(t)/h$; (c) maximum of $A_{1,0}(t)/h$; (d) maximum of $A_{3,0}(t)/h$; (e) maximum of $A_{5,0}(t)/h$. ——, Stable solutions; – – –, unstable solutions.

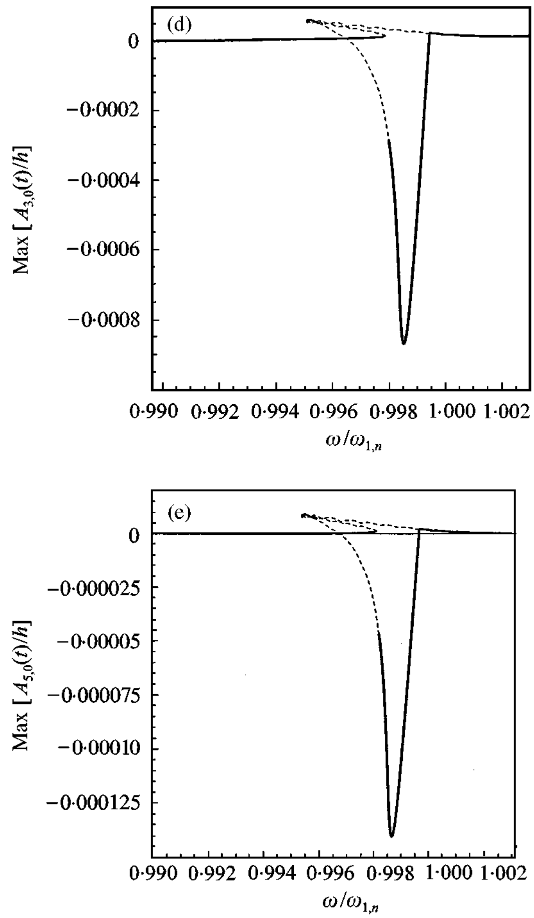

Figure 3. Continued.

non-linear shell response with sufficient accuracy. In general, it is resonably believed that, for the mth mode, all the axisymmetric modes with odd number of axial half-waves up to $2m + 1$ are necessary for an accurate computation of the shell response.

Figure 6 shows the response of the shell subjected to a modal excitation of fixed frequency, $\omega/\omega_{1,n} = 0{\cdot}999$, and increasing force amplitude. This figure is important because it shows that, even if for the case considered the softening behaviour is particularly weak, important non-linear phenomena arise at a relatively small vibration amplitude, namely 0·2 times the shell thickness h. In fact, Figure 6(a) shows that the vibration amplitude increases very rapidly from 0·2 to 0·6 h with a very modest force increment. After this point, an increase in the vibration amplitude needs a large force increment. In particular, at the bifurcation point, where the companion mode becomes active [see Figure 6(b)], there is a significant decrement of the vibration amplitude of the driven mode corresponding to a force increment; however, energy is transferred to the companion mode, the amplitude of which increases very quickly. These phenomena indicate that it is very restrictive to

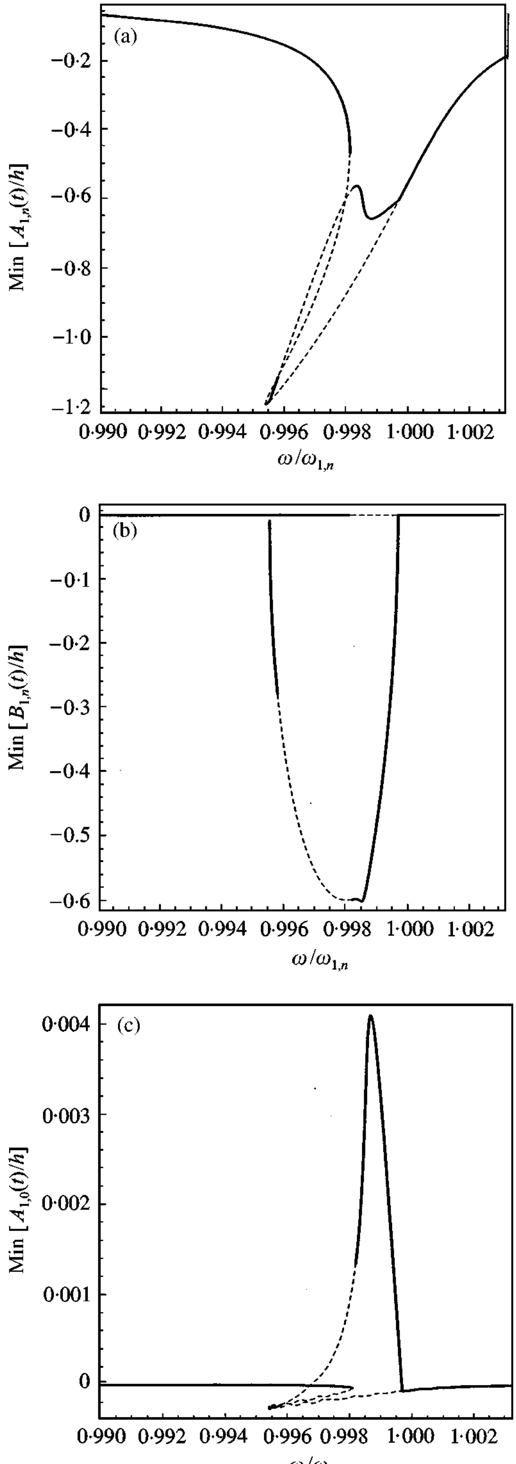

Figure 4. Frequency-response curve with companion mode participation, $m = 1$. (a) Minimum of $A_{1,n}(t)/h$; (b) minimum of $B_{1,n}(t)/h$; (c) minimum of $A_{1,0}(t)/h$; (d) minimum of $A_{3,0}(t)/h$; (e) minimum of $A_{5,0}(t)/h$. ——, Stable solutions; – – –, unstable solutions.

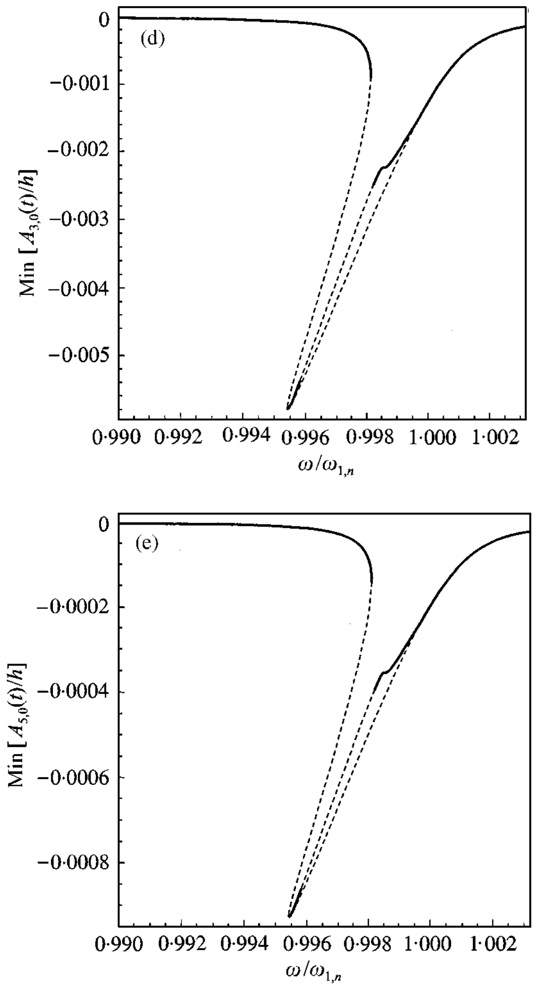

Figure 4. Continued.

study non-linear shell vibrations by considering only the backbone curve, pertaining to free vibrations. After all, the backbone curve indicates only the trend of non-linearity; in many cases, this is but minor phenomenon compared to other interesting results associated with large-amplitude shell vibrations.

4. FLUID-FILLED SHELLS

A case presenting a much stronger non-linearity is the one for which stability has been studied in Part I of the present study [11]. It is a circular cylindrical shell, simply supported at the ends ($N_x = 0$), water-filled, and having the following characteristics: $L/R = 2$, $h/R = 0{\cdot}01$, $E = 206 \times 10^9$ Pa, $\rho = 7850\ \text{kg/m}^3$, $\rho_F = 1000\ \text{kg/m}^3$ and $\nu = 0{\cdot}3$. In this case, no fluid flow is considered, and the model of

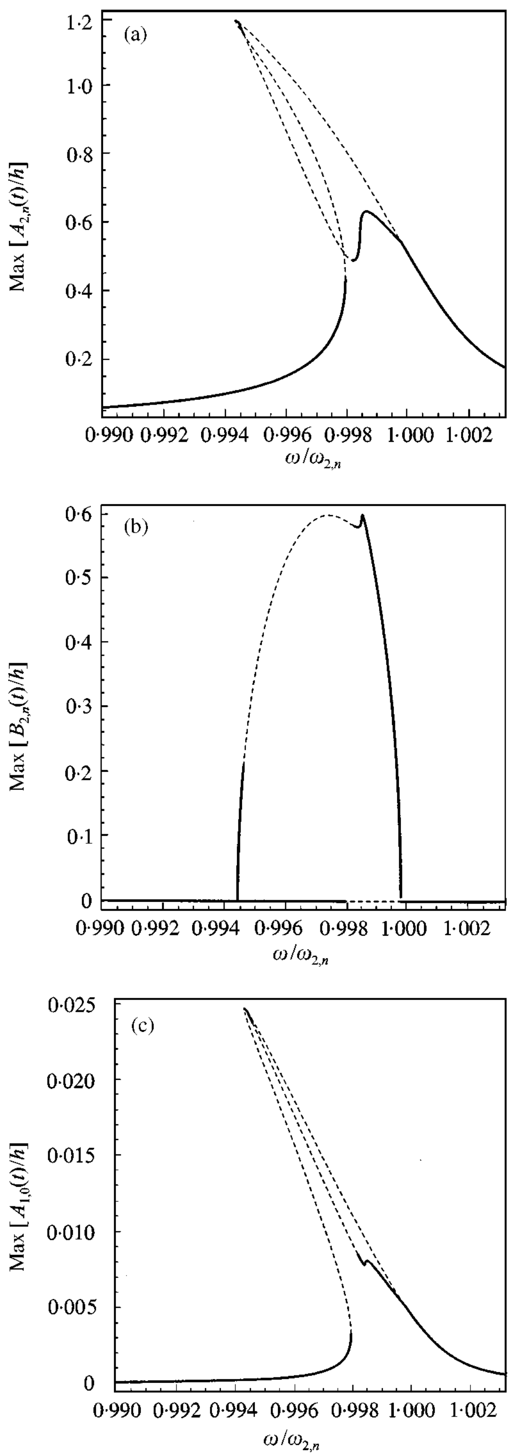

Figure 5. Frequency-response curve with companion mode participation, $m = 2$. (a) Maximum of $A_{2,n}(t)/h$; (b) maximum of $B_{2,n}(t)/h$; (c) maximum of $A_{1,0}(t)/h$; (d) maximum of $A_{3,0}(t)/h$; (e) maximum of $A_{5,0}(t)/h$. ——, Stable solutions; – – –, unstable solutions.

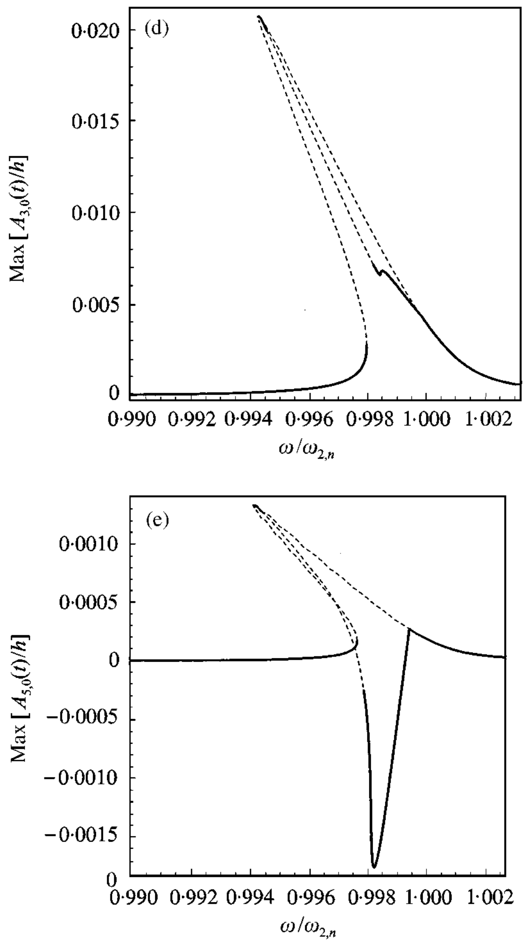

Figure 5. Continued.

Païdoussis and Denise [11], used to model the fluid–structure interaction, corresponds to a shell with open ends [15]. Here a linear potential fluid theory has been used; the accuracy of this assumption has been investigated by Gonçalves and Batista [10] and Lakis and Laveau [16]. The mode considered is $n = 5, m = 1$, with a damping ratio $\zeta_{1,n} = 0{\cdot}01$, a linear radian frequency $\omega_{1,n} = 2\pi \times 106{\cdot}69$ rad/s and an amplitude of the external modal excitation $f_{1,n} = 0{\cdot}03h\omega_{1,n}^2 m_1 [2/(\pi L)]$, where m_1 is defined after equation (46a) in Part I of the present study [11] and is related to the modal mass of the system.

The frequency-response relationship with companion mode participation is given in Figure 7, which shows only the first two generalized co-ordinates. In fact, all the generalized co-ordinates are qualitatively quite similar to the results presented in Figure 3, with a large change in the scale of the abscissa. In this case, the softening behaviour of the system is very significant. In general, the fluid–structure interaction of closed circular cylindrical shells containing dense

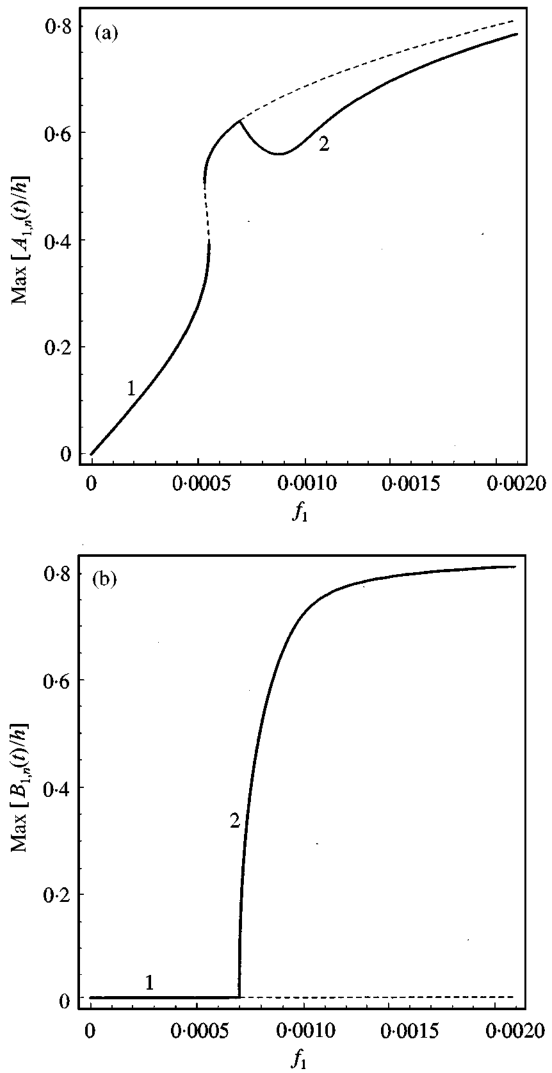

Figure 6. Frequency-response curve with companion mode participation, excitation frequency $\omega/\omega_{1,n} = 0{\cdot}999$ and $m = 1$. (a) Maximum of $A_{1,n}(t)/h$; (b) maximum of $B_{1,n}(t)/h$. ——, Stable solutions; – – –, unstable solutions.

fluids enhances the softening behaviour of the empty shell, as already observed in references [4, 10]. Moreover, there appears an interesting peak in the stable response of the driven and companion mode for $\omega/\omega_{1,n} \cong 0{\cdot}99$. This is due to the increased damping with respect to the case studied in Figure 3.

Figure 8 shows the time response of the system for excitation frequency $\omega/\omega_{1,n} = 0{\cdot}99$; it has been obtained by direct integration of the equations of motion, performed by using an adaptive step-size Runge–Kutta integration scheme. This figure is important for studying the phase relationships among the five generalized co-ordinates. Comparing Figures 8(a) and (b), a phase difference of $\pi/2$ between the driven mode and the companion mode is found. Moreover, the frequency of the

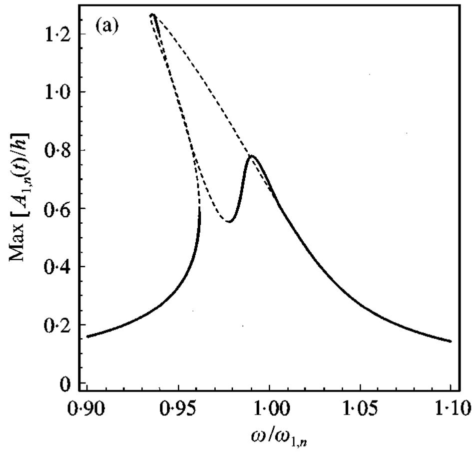

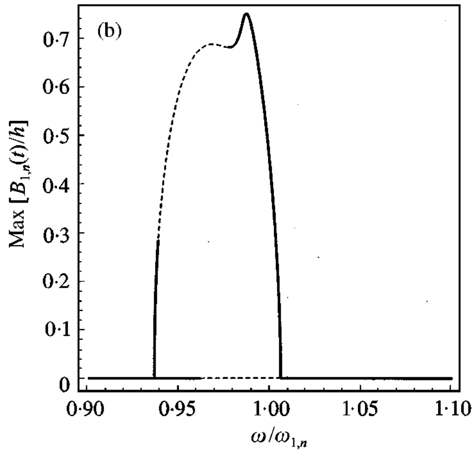

Figure 7. Frequency-response curve with companion mode participation for the fluid-filled shell, $m = 1$. (a) Maximum of $A_{1,n}(t)/h$; (b) maximum of $B_{1,n}(t)/h$. ——, Stable solutions; – – –, unstable solutions.

axisymmetric modes, Figure 8(c–e), is twice that for the driven and companion modes.

Another very interesting phenomenon is that no stable solutions exist for $0{\cdot}9616 < \omega/\omega_{1,n} < 0{\cdot}9779$. The Poincaré maps obtained for the five generalized co-ordinates for $\omega/\omega_{1,n} = 0{\cdot}97$ are given in Figure 9 and show a limit cycle; they have been obtained by direct integration of the equations of motion, performed by using an adaptive step-size Runge–Kutta integration scheme. These Poincaré maps are obtained by using the computed points corresponding to the instant where the force amplitude is maximum. The response in correspondence to the limit cycle contains an amplitude modulation, as observed in Figure 10(a) which shows the time response $A_{1,n}(t)$; the fundamental radian frequency of the modulation is $0{\cdot}0152 \times \omega_{1,n}$ rad/s. The limit cycle is an attractive monodimensional set embedded in 10-dimensional phase space in the Poincaré map. The response is not chaotic as observed in the frequency spectrum given in Figure 10(b). It shows that the single frequency response obtained in the stable region is divided into several close

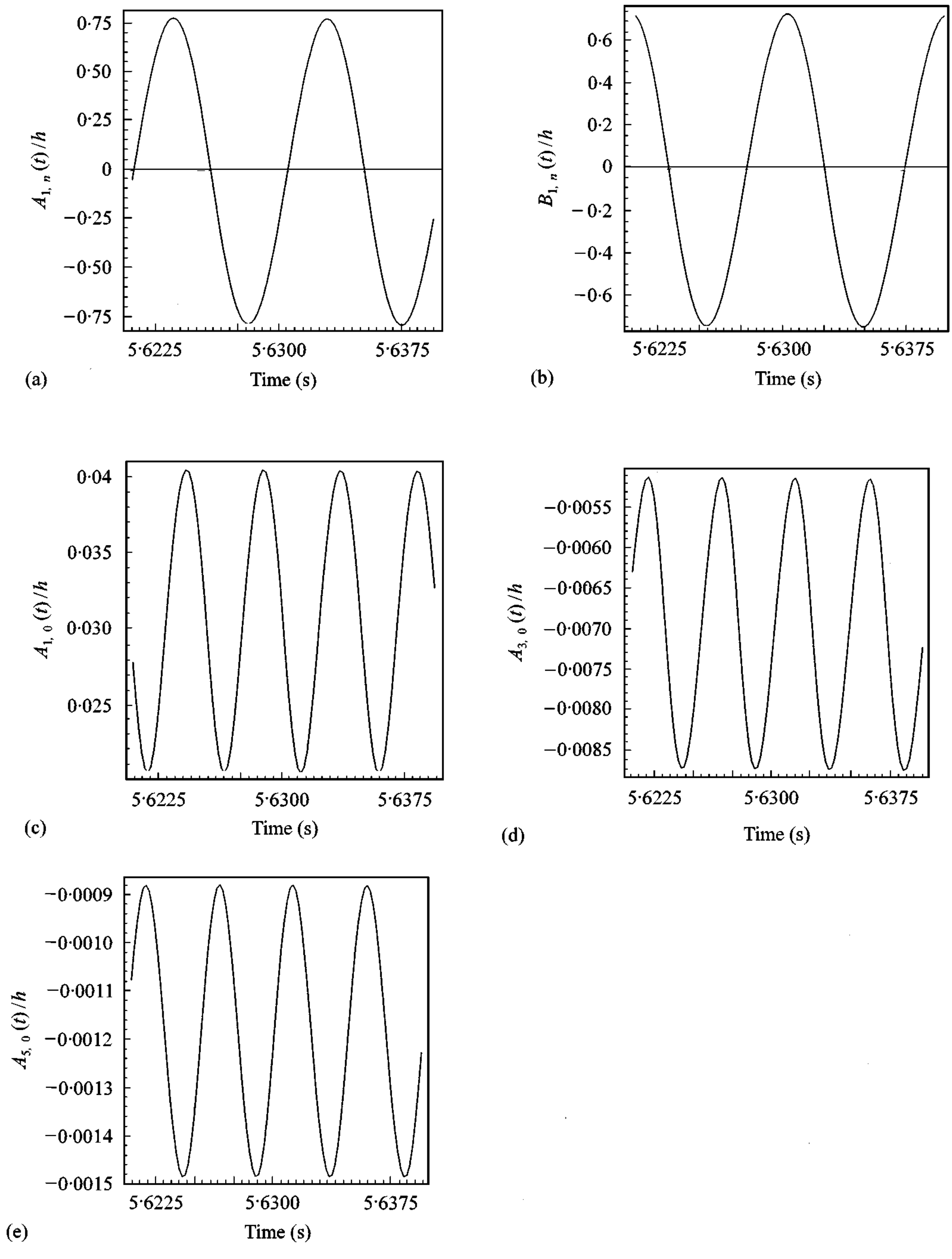

Figure 8. Time response of the fluid-filled shell; $\omega/\omega_{1,n} = 0{\cdot}99$ and $f_{1,n} = 0{\cdot}03 h\omega_{1,n}^2 m_1[2/(\pi L)]$. (a) $A_{1,n}(t)/h$; (b) $B_{1,n}(t)/h$; (c) $A_{1,0}(t)/h$; (d) $A_{3,0}(t)/h$; (e) $A_{5,0}(t)/h$.

frequencies that give a beating phenomenon. The whole area where no stable solutions exist is associated with beating phenomena that give modulations in the oscillation amplitude. Note that the small portion of the spectrum, represented in

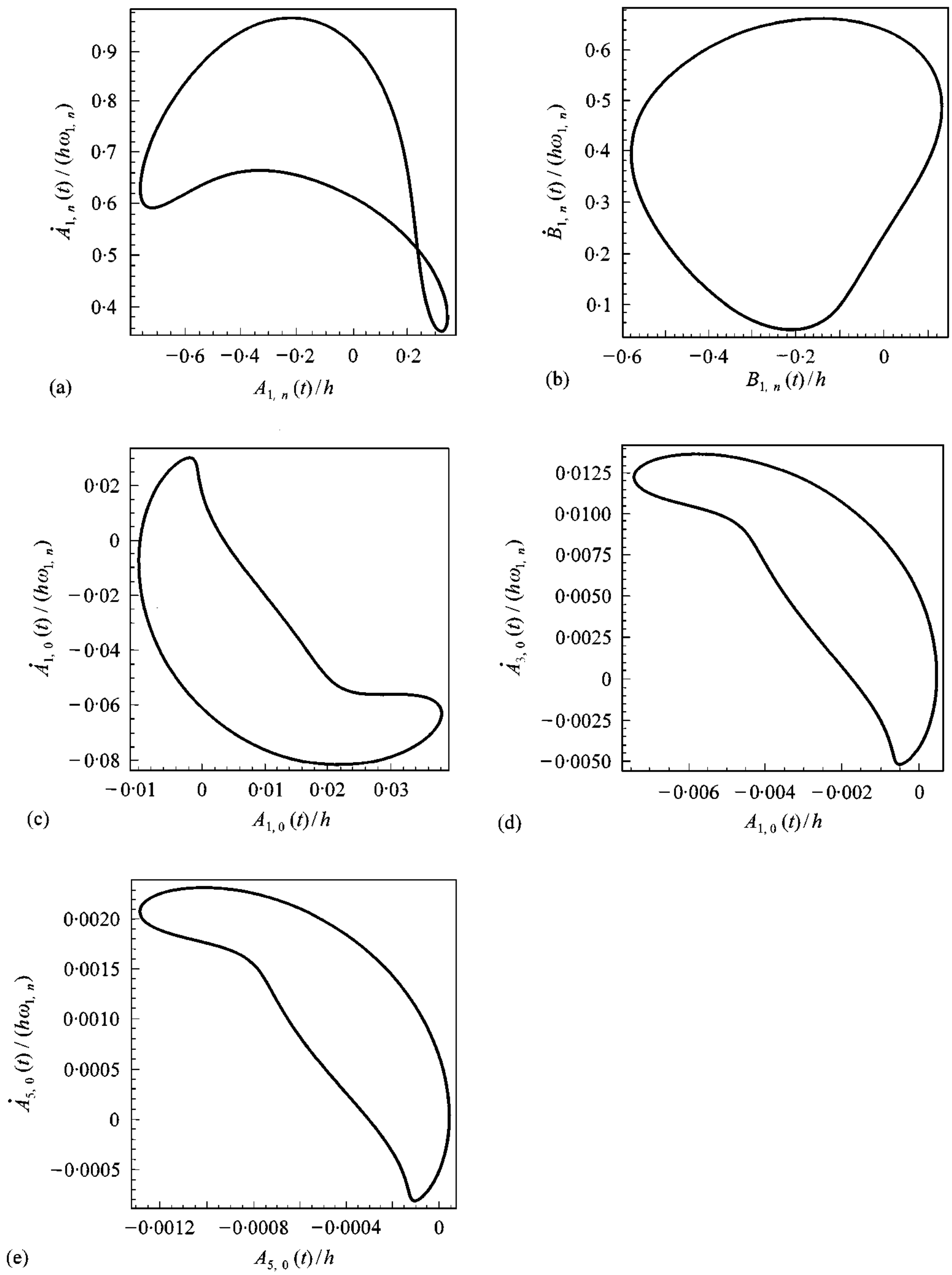

Figure 9. Poincaré maps for $\omega/\omega_{1,n} = 0{\cdot}97$ and $f_{1,n} = 0{\cdot}03h\omega_{1,n}^2 m_1[2/(\pi L)]$ showing limit-cycle motion; fluid filled shell, $m = 1$. (a) First generalized co-ordinate; (b) second generalized co-ordinate; (c) third generalized co-ordinate; (d) fourth generalized co-ordinate; (e) fifth generalized co-ordinate.

Figure 10(b), contains most of the energy of the time signal, i.e., no harmonic components are present at lower and higher frequencies. Analogous results are obtained for the other generalized co-ordinates; in particular, the response of the

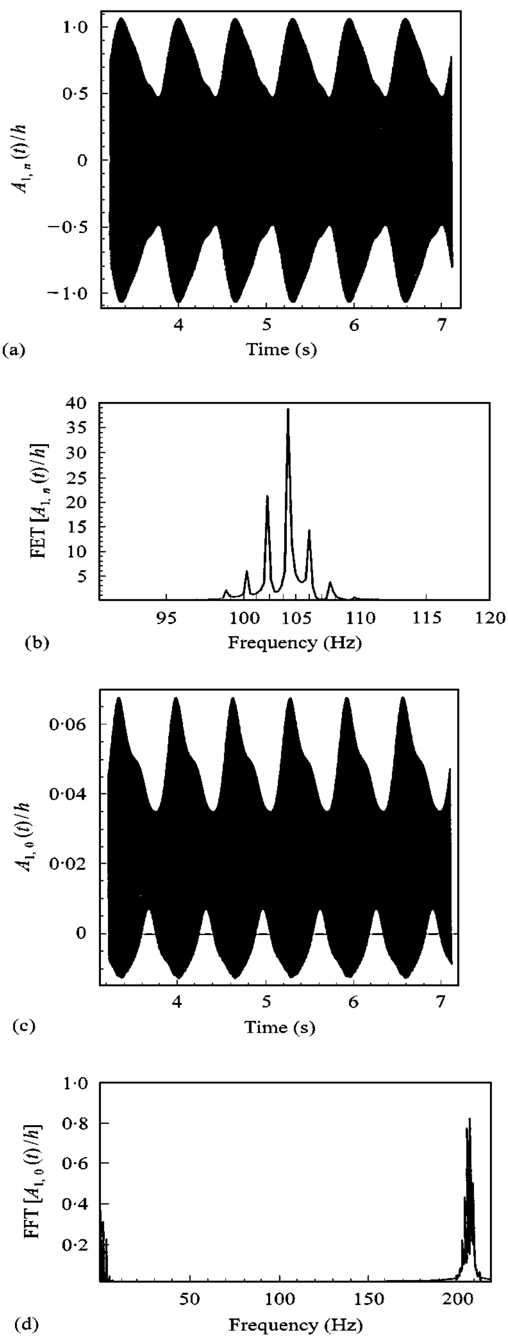

Figure 10. Response in correspondence to the limit cycle; $\omega/\omega_{1,n} = 0{\cdot}97$ and $f_{1,n} = 0{\cdot}03h\omega_{1,n}^2 m_1 [2/(\pi L)]$. (a) Time history $A_{1,n}(t)$; (b) frequency analysis of $A_{1,n}(t)$; (c) time history $A_{1,0}(t)$; (d) frequency analysis of $A_{1,0}(t)$.

first axisymmetric mode $A_{1,0}(t)$ is shown in Figure 10(c) and its spectrum is given in Figure 10(d). The spectrum shows that the axisymmetric mode has twice the frequency of the asymmetric modes, as already observed in previous studies [4, 9].

5. CONCLUSIONS

The present study indicates that it is limited to study non-linear shell vibrations by considering only the backbone curve, pertaining to free vibrations, since this only indicates the trend of non-linearity; in many cases, this is just one of the many interesting phenomena associated with large-amplitude shell vibrations. Strong non-linear phenomena arise at relatively small vibration amplitudes, and the appearance of the companion mode at a vibration amplitude of around 0·6 times the shell thickness complicates the shell response. Non-linear phenomena are enhanced by fluid–structure interaction with dense, stationary fluids.

The trend of non-linearity is generally of softening type. It is reasonably believed that all the axisymmetric modes with odd number of axial half-waves up to $2m + 1$, where m is the number of axial half-waves of the mode investigated, are necessary for an accurate computation of the shell response.

The present study could be improved by using a more refined non-linear shell theory [9, 16, 17] instead of the non-linear Donnell shallow shell one, as discussed in Part I of the present study where the theory is presented. However, the cases studied satisfy the conditions of applicability of shallow-shell theory. It could be interesting to verify the effect of additional asymmetric modes with a number of circumferential waves a multiple of n and an odd number of longitudinal waves in the expansion of the shell flexural displacement, as discussed by Ginsberg [7]. However, these are not expected to have the same fundamental effect on the trend of non-linearity as the first and third axisymmetric modes, definitively investigated here.

ACKNOWLEDGMENTS

This work was partially supported by a grant of the Italian Space Agency (ASI). M. P. Païdoussis also expresses his gratitude to NSERC of Canada and FCAR of Québec for their support.

REFERENCES

1. E. H. Dowell, 1998 *Journal of Fluids and Structures* **12**, 1087–1089. Comments on the nonlinear vibrations of cylindrical shells.
2. M. Amabili, F. Pellicano and M. P. Païdoussis 1999 *Journal of Fluids and Structures* **13**, 159–160. Further comments on the nonlinear vibrations of cylindrical shells.
3. D. A. Evensen 1999 *Journal of Fluids and Structures* **13**, 161–164. Nonlinear vibrations of cylindrical shells—logical rationale.
4. M. Amabili, F. Pellicano and M. P. Païdoussis 1998 *Journal of Fluids and Structures* **12**, 883–918. Nonlinear vibrations of simply supported, circular cylindrical shells, coupled to quiescent fluid.
5. D. A. Evensen 1967 *NASA TN D*-4090. Nonlinear flexural vibrations of thin-walled circular cylinders.
6. E. H. Dowell and C. S. Ventres 1968 *International Journal of Solids and Structures* **4**, 975–991. Modal equations for the nonlinear flexural vibrations of a cylindrical shell.
7. J. H. Ginsberg 1973 *Journal of Applied Mechanics* **40**, 471–477. Large amplitude forced vibrations of simply supported thin cylindrical shells.

8. J. C. Chen and C. D. Babcock 1975 *AIAA Journal* **13**, 868–876. Nonlinear vibration of cylindrical shells.
9. M. Ganapathi and T. K. Varadan 1996 *Journal of Sound and Vibration* **192**, 1–14. Large amplitude vibrations of circular cylindrical shells.
10. P. B. Gonçalves and R. C. Batista 1988 *Journal of Sound and Vibration* **127**, 133–143. Non-linear vibration analysis of fluid-filled cylndrical shells.
11. M. Amabili, F. Pellicano and M. P. Païdoussis 1999 *Journal of Sound and Vibration* **225**, 655–699. Nonlinear dynamics and stability of circular cylindrical shells containing flowing fluid, Part I: stability.
12. E. J. Doedel, A. R. Champneys, T. F. Fairgrieve, Y. A. Kuznetsov, B. Sandstede and X. Wang 1998 *Auto*97: *Continuation and Bifurcation Software for Ordinary Differential Equations* (*with HomCont*). Montreal, Canada: Concordia University.
13. S. Atluri 1972 *International Journal of Solids and Structures* **8**, 549–569. A perturbation analysis of non-linear free flexural vibrations of a circular cylindrical shell.
14. T. K. Varadan, G. Prathap and H. V. Ramani 1989 *AIAA Journal* **27**, 1303–1304. Nonlinear free flexural vibration of thin circular cylindrical shells.
15. M. Amabili 1997 *Transactions of the ASME*, *Journal of Vibration and Acoustics* **119**, 476–484. Flexural vibration of cylindrical shells partially coupled with external and internal fluids.
16. A. A. Lakis and A. Laveau 1991 *International Journal of Solids and Structues* **28**, 1079–1094. Non-linear dynamic analysis of anisotropic cylindrical shells containing a flowing fluid.
17. A. Selmane and A. A. Lakis 1997 *Journal of Sound and Vibration* **202**, 67–93. Non-linear dynamic analysis of orthotropic open cylindrical shells subjected to a flowing fluid.